

# JCTC

Journal of Chemical Theory and Computation

## Spectroscopic Properties of Formaldehyde in Aqueous Solution: Insights from Car–Parrinello and TDDFT/CASPT2 Calculations

Paola Lupieri,<sup>†,‡,§</sup> Emiliano Ippoliti,<sup>†,‡</sup> Piero Altoè,<sup>||</sup> Marco Garavelli,<sup>||</sup> M. Mwalaba,<sup>⊥,∇</sup>  
and Paolo Carloni<sup>\*,†,‡,§,¶</sup>

*German Research School for Simulation Sciences GmbH, 52425 Jülich and RWTH Aachen, Germany, SISSA, via Bonomea 265, 34136 Trieste, Italy, Department of Chemistry “G. Ciamician”, University of Bologna, via Selmi 2, I-40126 Bologna, Italy, International Centre for Theoretical Physics (ICTP), Strada Costiera 11, 34151 Trieste, Italy, and Democritos Modeling Center for Research in Atomistic Simulation, via Bonomea 265, 34136 Trieste, Italy*

Received July 9, 2010

**Abstract:** We present Car–Parrinello and Car–Parrinello/molecular mechanics simulations of the structural, vibrational, and electronic properties of formaldehyde in water. The calculated properties of the molecule reproduce experimental values and previous calculations. The  $n \rightarrow \pi^*$  excitation energy, calculated with TDDFT and CASPT2, agrees with experimental data. In particular, it shows a blue shift on going from the gas phase to aqueous solution. Temperature and wave function polarization contributions have been disentangled.

### Introduction

The carbonyl group is a key component of (bio)organic molecules, with interesting optical properties. As we know from textbooks, the oxygen's electron lone pairs form nonbonding orbitals ( $n$ ), whose electrons can be promoted to an antibonding  $\pi$  orbital localized over the C=O bond. In the ground states of many carbonyl compounds, the  $n$  state is the highest energy occupied molecular orbital (HOMO).<sup>1</sup> In that case, the lowest transition energy is the singlet–singlet transition  $n \rightarrow \pi^*$ .

Formaldehyde, the simplest system containing such functionality, has been a test case for quantitative prediction of this transition (and recently also of the corresponding

emission<sup>2,3</sup>) in the isolated molecule and aqueous solution. The approaches used range from semiempirical AM1,<sup>4</sup> first-principle DFT,<sup>5–7</sup> ab initio HF,<sup>8,9</sup> and to post-HF techniques such as CISD and CASSCF<sup>6,10–18</sup> for formaldehyde using either molecular mechanics in a QM/MM scheme,<sup>4,6,9–13,17,18</sup> an implicit solvent,<sup>5,19,20</sup> or full quantum representation<sup>7,15,16</sup> for the solvent (see the Supporting Information for details).

In the gas phase (at 0 K), the calculated values range between 3.3 and 4.5 eV. This may be compared with the experimental values measured at 330 K, ranging from 3.3 to 5 eV, with a maximum around 3.8 eV.<sup>21,22</sup>

In solution, at room temperature (298 or 300 K), these computational approaches predict values in the range 3.5–5.7 eV, indicating a blue shift due to the solvent as well as the temperature between 0.07 and 0.43 eV. Experimentally, formaldehyde undertakes a reaction in water, forming methyleneglycol<sup>23</sup>



Since the equilibrium constant of the reaction is  $10^4$ , the absorption cannot be measured in submolar solutions. However, it can be detected in highly concentrated solutions (10 M or more) at about 4.2 eV,<sup>23</sup> where molecular clusters

\* Corresponding author e-mail: p.carloni@grs-sim.de.

<sup>†</sup> German Research School for Simulation Sciences.

<sup>‡</sup> RWTH Aachen.

<sup>§</sup> SISSA.

<sup>||</sup> University of Bologna.

<sup>⊥</sup> ICTP.

<sup>¶</sup> Democritos Modeling Center for Research in Atomistic Simulation.

<sup>∇</sup> Permanent address: Department of Physics, University of Zambia, School of Natural Sciences, Lusaka 10101, Zambia.

of formaldehyde are likely to exist. The spectra are likely to retain the properties of a single formaldehyde solvated molecule.<sup>7,9,11–16</sup> Thus, these experimental findings are consistent with a solvent blue-shift effect.

Ab initio Car–Parrinello (CP) molecular dynamics (MD) and hybrid CPMD/MM calculations in conjunction with techniques for excited states such as time-dependent density functional theory (TDDFT)<sup>24,25</sup> are mature techniques to study electronic absorption spectra of solutes in water at room temperature.<sup>26–29</sup> Ab initio MD allows realistic simulations to be performed without adjustable parameters, which is a necessary drawback of empirical approaches and continuum methods. In addition, it allows for an explicit description of H bonding, whose polarization effects might be difficult to be captured in continuum models.<sup>25</sup>

Here we use such approaches to investigate formaldehyde in water. The effects of the environment on the structural and electronic properties of formaldehyde are discussed in detail. Excitation energies are computed using not only TDDFT<sup>30</sup> but also complete active space with second-order perturbation theory (CASPT2).<sup>31</sup> CASPT2 has been already widely used as a reference for high-level calculations, and it has been applied in the past to study solvent effects on carbonyl-bearing molecules.<sup>2,32–34</sup> The calculations are run over a set of snapshots extracted from the simulations.

## Computational Methods

The quantum problem was solved within the framework of DFT,<sup>35,36</sup> using the BLYP gradient-corrected functional.<sup>37,38</sup> This provides good geometrical features and has been shown to treat H-bonded systems with fairly good accuracy.<sup>39–42</sup> The absorption spectrum of formaldehyde in the gas phase was computed also with the PBE functional,<sup>43</sup> which is known from the literature to reproduce absorption energies with good accuracy.<sup>44</sup>

The wave functions were expanded on a plane wave basis set, up to a cutoff of 70 Ry. The atomic all-electrons potentials were substituted with norm-conserving Troullier–Martins pseudopotentials,<sup>45</sup> and the Kleinman–Bylander approach was used to treat their nonlocal part.<sup>46</sup> The simulations were run with dispersion-corrected pseudopotentials,<sup>47</sup> which are shown to reproduce quite well London forces.

The in vacuo geometry of formaldehyde ( $\mathbf{FA}_{\text{opt}}$  hereafter) was optimized using the GDIIS algorithm<sup>48</sup> up to a variation of the gradient on the nuclei positions of  $10^{-6}$  au and on the wave function of  $10^{-8}$  au.

DFT CPMD simulations for formaldehyde in vacuo ( $\mathbf{FA}_{\text{CPMD}}$  hereafter) and in water ( $\mathbf{FA}_{\text{CPMD}}^{\text{aq}}$ ) as well as hybrid CPMD/MM simulations<sup>24</sup> for formaldehyde in water ( $\mathbf{FA}_{\text{QM/MM}}^{\text{aq}}$ ) were carried out. In the latter scheme, the QM part was given by the formaldehyde molecule and the MM part by water. The second was described with the TIP3P model.<sup>49</sup>

Formaldehyde was inserted in a box of edges  $9.01 \text{ \AA} \times 7.39 \text{ \AA} \times 8.65 \text{ \AA}$  ( $\mathbf{FA}_{\text{opt}}$ ), in a water box of edges  $11.33 \text{ \AA} \times 11.22 \text{ \AA} \times 9.63 \text{ \AA}$  ( $\mathbf{FA}_{\text{CPMD}}^{\text{aq}}$ ), and in a box of  $8.8 \text{ \AA} \times 9.3 \text{ \AA} \times 8.8 \text{ \AA}$  ( $\mathbf{FA}_{\text{QM/MM}}^{\text{aq}}$ ). In  $\mathbf{FA}_{\text{CPMD}}^{\text{aq}}$ , the box contained 43 water molecules (density =  $1.09 \text{ g/cm}^3$ ). In  $\mathbf{FA}_{\text{QM/MM}}^{\text{aq}}$ , the

QM simulation box was further inserted in a  $28.4 \text{ \AA} \times 26.1 \text{ \AA} \times 28.9 \text{ \AA}$  orthorhombic box of 697 water molecules (density =  $1.03 \text{ g/cm}^3$ ). Both  $\mathbf{FA}_{\text{CPMD}}^{\text{aq}}$  and  $\mathbf{FA}_{\text{QM/MM}}^{\text{aq}}$  were first equilibrated by classical MD (1 ns classical MD was performed in the NPT ensemble ( $T = 300 \text{ K}$ ,  $P = 1 \text{ atm}$ ), obtained using a Langevin-like thermostat and barostat,<sup>50</sup> using a time step of 1 fs and periodic boundary conditions. Interactions were described with the parm99 force field<sup>51</sup> and the TIP3P model of water molecules.<sup>49</sup> The lengths of bonds involving a hydrogen were constrained with the Shake algorithm.<sup>52</sup> The PME algorithm was adopted to treat electrostatic interactions.<sup>53</sup> A cutoff of  $14 \text{ \AA}$  was set for van der Waals interactions and the real part of the Coulomb interactions. The MD was run with the software NAMD.<sup>54</sup>)

In  $\mathbf{FA}_{\text{opt}}$ ,  $\mathbf{FA}_{\text{CPMD}}$ , and  $\mathbf{FA}_{\text{QM/MM}}^{\text{aq}}$ , isolated system conditions within the plane-wave formalism were achieved with the scheme of Martyna and Tuckerman.<sup>55</sup>

$\mathbf{FA}_{\text{CPMD}}$ ,  $\mathbf{FA}_{\text{CPMD}}^{\text{aq}}$ , and  $\mathbf{FA}_{\text{QM/MM}}^{\text{aq}}$  underwent 3, 3, and 12 ps of MD, respectively. These simulations were performed in the NVT ensemble at 300 K. Constant temperature conditions were applied through a Nosé–Hoover chain of thermostats.<sup>56</sup>  $\mathbf{FA}_{\text{CPMD}}$  also underwent geometry optimization prior to the dynamics (same procedure as for  $\mathbf{FA}_{\text{opt}}$ ).

**Calculated Properties.** (1) The dipole moment of  $\mathbf{FA}_{\text{opt}}$  was computed from real-space integration in the isolated cell.<sup>57</sup> The vibrational normal modes of the molecule were calculated from the diagonalization of the Hessian matrix. This was calculated using the finite difference technique with a step size of 0.01 bohr and a convergence criterion of  $10^{-8}$  au over the wave function gradient.

The dipole moment of formaldehyde in  $\mathbf{FA}_{\text{CPMD}}^{\text{aq}}$  and  $\mathbf{FA}_{\text{QM/MM}}^{\text{aq}}$  was computed from the positions of the nuclei and those of the Wannier centers of the molecule,<sup>58,59</sup> calculated every 50 steps of the dynamics. The vibrational spectrum of formaldehyde was obtained from the Fourier transform of the autocorrelation of the velocities of its atoms,<sup>60</sup> also in this case calculated every 50 steps of the dynamics. Normal mode vibrations were derived projecting this spectrum on the normal modes of the isolated molecule.<sup>61</sup>

(2) The radial distribution functions (rdf) of water oxygens and hydrogens around formaldehyde's oxygen in  $\mathbf{FA}_{\text{CPMD}}^{\text{aq}}$  and  $\mathbf{FA}_{\text{QM/MM}}^{\text{aq}}$  were calculated up to one-half the smallest dimension of the simulation box, discretized in steps of  $0.05 \text{ \AA}$ , and taking periodic boundary conditions into account.

(3) The first electronic excitations were obtained by TDDFT<sup>62</sup> and CASPT2<sup>31</sup> calculations. They were calculated on  $\mathbf{FA}_{\text{opt}}$  and on 100 equispaced snapshots from  $\mathbf{FA}_{\text{CPMD}}$ ,  $\mathbf{FA}_{\text{CPMD}}^{\text{aq}}$ , and  $\mathbf{FA}_{\text{QM/MM}}^{\text{aq}}$  simulations. Casida's formulation of the linear-response TDDFT<sup>63</sup> was used to perform the direct calculation of the electronic excitations on the molecule. The Tamm–Dancoff approximation was applied in this case.<sup>30</sup>

CASPT2 calculations exploited a zeroth-order CASSCF wave function with no IPEA shift. Here, the complete active space included 4 electrons and 3 orbitals ( $n$ ,  $\pi$ , and  $\pi^*$ ). This active space was chosen after careful tests and turned out to be the best compromise between accuracy and reliability. The wave function was expanded over the ANO-S basis set<sup>64</sup> with contraction 7s6p3d for carbon and oxygen and 4s3p for hydrogen.

Table 1

	$\mathbf{FA}_{\text{opt}}$ (BLYP)	$\mathbf{FA}_{\text{opt}}$ (PBE)	exp.	$\mathbf{FA}_{\text{CPMD}}$	$\mathbf{FA}_{\text{CPMD}}^{\text{aq}}$	$\mathbf{FA}_{\text{QM/MM}}^{\text{aq}}$
$d(\text{C}=\text{O})$ (Å)	1.22	1.22	1.20 <sup>a</sup>	$1.23 \pm 0.01$	$1.23 \pm 0.01$	$1.22 \pm 0.01$
$d(\text{C}-\text{H})$ (Å)	1.12	1.12	1.10 <sup>a</sup>	$1.12 \pm 0.01$	$1.11 \pm 0.01$	$1.11 \pm 0.01$
$\angle(\text{HCH})$ (deg)	116	116	116 <sup>a</sup>	$116 \pm 1$	$117 \pm 2$	$117 \pm 2$
$\mu$ (D)	2.30	2.25	2.34 <sup>b</sup>	$2.86 \pm 0.16$	$3.72 \pm 0.29$	$3.45 \pm 0.25$

<sup>a</sup> Value from ref 70. <sup>b</sup> Value from ref 72.

CASPT2 and TDDFT calculations of the solute in the presence of the solvent field were calculated for  $\mathbf{FA}_{\text{QM/MM}}^{\text{aq}}$  (and also  $\mathbf{FA}_{\text{CPMD}}^{\text{aq}}$  for the CASPT2 calculations) following refs 24, 30, and 65.

All DFT and TDDFT calculations were performed with the BLYP functional.<sup>37,38</sup> The calculations at 0 K were also performed at the PBE level.<sup>43</sup> All DFT and TDDFT calculations were performed with the CPMD code.<sup>57</sup> The code was interfaced with the Gromos classical MD program<sup>66</sup> in  $\mathbf{FA}_{\text{QM/MM}}^{\text{aq}}$ . The CASSCF/CASPT2 calculations were performed with the Molcas program.<sup>67</sup> Here, the solvent was introduced as a perturbation of the CASPT2 wave function by the point charges of the water molecules solvating formaldehyde. No charge screening was applied. The classical van der Waals contributions were not included.

## Results and Discussion

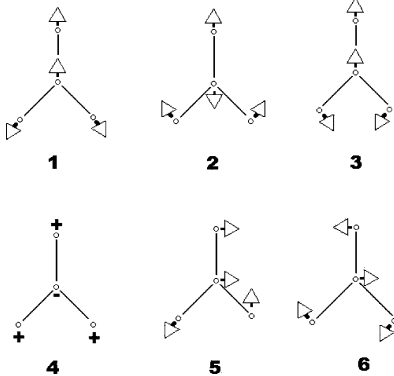
**Ground State.** The geometrical features of formaldehyde in vacuo calculated using the BLYP<sup>37,38</sup> and the PBE<sup>43</sup> functionals are the same (Table 1). They are similar to those obtained by DFT-B3LYP,<sup>68,69</sup> MRCI,<sup>18</sup> CASSCF, and CCSD calculations<sup>10,14</sup> (Table S4 in the Supporting Information). The bond lengths are slightly longer than those observed based on microwave spectra,<sup>70,71</sup> whereas the bond angle is the same (Table 1). Formaldehyde is a planar molecule. Its symmetry elements are those of the  $C_{2v}$  point symmetry group: one  $C_2$  axis (passing through the carbon and oxygen atoms and bisecting the HCH angle) and two  $\sigma_v$  planes (the molecular plane and the plane perpendicular to it, bisecting the HCH angle). Here, we report formaldehyde's structural determinants and dipole moment from our simulations and from the literature. Our calculations are at the DFT/BLYP level, unless otherwise specified.

The calculated dipole moment  $\bar{\mu}$  (Table 1) is aligned with the  $\text{O}=\text{C}$  bond and has a modulus  $\mu = 2.25\text{--}2.3$  D, in accordance with DFT-B3LYP<sup>6,7</sup> and PBE0,<sup>5</sup> CASSCF,<sup>10,12</sup> MRCI,<sup>18</sup> as well as CCSD calculations<sup>11</sup> (Table S5 in the Supporting Information). It is also in agreement with the value obtained by microwave spectroscopy.<sup>72</sup>

The frequencies of the calculated normal modes (Table 2) agree within  $50\text{--}100\text{ cm}^{-1}$  with B3LYP calculations,<sup>68,69</sup> whereas they are rather far from the CASSCF results of ref 10 (shifts of  $50\text{--}500\text{ cm}^{-1}$ ). However, it is known from the literature<sup>73</sup> that CAS-calculated vibrational frequencies are overestimated, due to the lack of electronic correlation, and that a scaling factor of 0.9 should be applied. Our calculations agree within  $70\text{ cm}^{-1}$  with experimental data<sup>71</sup> (Table 2).

We next analyze solvation and temperature effects on formaldehyde by performing DFT CPMD ( $\mathbf{FA}_{\text{CPMD}}^{\text{aq}}$ ) and hybrid CPMD/MM simulations<sup>24</sup> of formaldehyde in water ( $\mathbf{FA}_{\text{QM/MM}}^{\text{aq}}$ ) at 300 K.

**Table 2.** Frequencies of the Six Normal Modes of Formaldehyde<sup>68,74</sup> ( $\text{cm}^{-1}$ ) Calculated at the BLYP Level of Theory<sup>a</sup>



$C_{2v}$ -symmetric species	$A_1$			$B_1$		$B_2$	
	$\nu_1$	$\nu_2$	$\nu_3$	$\nu_4$	$\nu_5$	$\nu_6$	
exp.	2766	1746	1500	1167	2843	1251	
$\mathbf{FA}_{\text{opt}}$	2803	1736	1472	1144	2839	1174	
$\Delta\nu$ $\mathbf{FA}_{\text{CPMD}}$	-309	-104	-150	-75	-368	-117	
$\Delta\nu$ $\mathbf{FA}_{\text{CPMD}}^{\text{aq}}$	-100	-149	-98	-64	-85	-79	
$\Delta\nu$ $\mathbf{FA}_{\text{QM/MM}}^{\text{aq}}$	-180	-108	-61	-14	-188	12	

<sup>a</sup> Comparison is made with experimental data for formaldehyde in the gas phase.<sup>75</sup> Mode 1: symmetric C-H stretching. Mode 2: C=O stretching. Mode 3:  $\text{CH}_2$  bending. Mode 4:  $\text{CH}_2$  out of plane bending. Mode 5: antisymmetric C-H stretching. Mode 6:  $\text{CH}_2$  rocking.

Both temperature and solvation slightly affect the structural parameters. In both DFT CPMD and hybrid CPMD/MM simulations of formaldehyde in water ( $\mathbf{FA}_{\text{CPMD}}^{\text{aq}}$  and  $\mathbf{FA}_{\text{QM/MM}}^{\text{aq}}$ , respectively), the average  $\text{C}=\text{O}$  bond is elongated and the  $\text{C}-\text{H}$  bonds are shortened by about  $0.01\text{ Å}$ , which falls within our statistical uncertainty (see Table 1), and is therefore insignificant. The average value of  $\mu$  is instead remarkably larger than that of  $\mathbf{FA}_{\text{opt}}$  (more than 50%, see Table 1). Since the extent of the temperature and solvation effects on the structure is negligible, we conclude that in our approach the solvent affects the dipole moment intensity of formaldehyde by polarizing its electronic wave function, rather than by modifying its structure. This finding is in line with B3LYP/MM calculations on large clusters of water molecules around formaldehyde, which suggest that  $\mu$  increases by 42% on passing from the gas phase to water solution<sup>7</sup> (Table S5 in the Supporting Information). They are also consistent with CPMD/MM calculations of acetone in water, which predict the value of  $\mu$  to increase by about 60% upon going from the gas phase to aqueous solution.<sup>24</sup>

In both  $\mathbf{FA}_{\text{CPMD}}^{\text{aq}}$  and  $\mathbf{FA}_{\text{QM/MM}}^{\text{aq}}$ , the radial distribution function (rdf) between the carbonyl oxygen atom and water hydrogens exhibits a first peak around  $1.9\text{--}2.0\text{ Å}$  and a minimum around  $2.5\text{ Å}$  (Figure S2 and Table S6 in the



**Table 3.** Absorption Energies (in eV) of Formaldehyde in Vacuo<sup>a</sup>

	<b>FA<sub>opt</sub></b>	<b>FA<sub>CPMD</sub></b>
TDDFT (this work)	3.85, 3.82, <sup>b</sup> 3.89 <sup>c</sup>	3.77 ± 0.04
CASPT2 (this work)	3.84, 3.86 <sup>c</sup>	3.76 ± 0.05
PBE0(6-311G(d,p))// TD-PBE0(6-311++G(d,p)) <sup>5</sup>	3.84	
B3LYP(cc-pVTZ)//LR-B3LYP, LR-CCSD(6-31++G) <sup>6</sup>	3.81, 3.84	
exp./CASSCF(ANO) <sup>12</sup>	4.04	
MP2(cc-pvtz)// MRCI(cc-pvtz) <sup>18</sup>	4.04	
experimental values	3.79, <sup>21</sup> 3.86 <sup>22</sup>	

<sup>a</sup> Values are reported for the TDDFT and CASPT2 calculations performed in this work for formaldehyde at 0 and 300 K. The reported TDDFT values are referred to calculations at the BLYP level, unless otherwise specified. Experimental as well as some previous theoretical results are reported in the last 5 lines of the tables. Some details of the levels of theory of the cited calculations are indicated (ground-state geometry//absorption energy). See the Supporting Information for further details. <sup>b</sup> Calculation at the PBE level. <sup>c</sup> Calculation performed over the CASSCF-optimized structure of formaldehyde.

**Table 4.** Absorption Energies (in eV) of Formaldehyde in Water Solution<sup>a</sup>

	<b>FA<sub>CPMD</sub><sup>aq</sup></b>		<b>FA<sub>QMMM</sub><sup>aq</sup></b>	
	FF	0	FF	0
TDDFT		3.77 ± 0.04	4.0 ± 0.1	3.77 ± 0.07
CASPT2	4.08 ± 0.12	3.77 ± 0.05	4.07 ± 0.11	3.77 ± 0.09

<sup>a</sup> Columns "FF" (columns "0") indicate single-point calculations with water molecules taken explicitly into account (with water molecules removed). The reported TDDFT values are referred to calculations at the BLYP level.

Supporting Information). Integration of this peak up to the minimum yields a coordination number of about 1.9. Rather similar results are obtained from other QM and QM/MM techniques:<sup>4,9,10,15,16</sup> ref 4 predicts the peak of the oxygen–hydrogen rdf at 1.8 Å (integrating to 1.4 hydrogens), ref 15 at 1.7 Å (integrating to 1.9 hydrogens), and ref 16 at 1.9 Å. The oxygen–oxygen rdf (Table S6 in the Supporting Information) shows a first peak around 2.9–3.0 Å; integration up to the first minimum of the distribution gives a value of 2.5 and 2.9 water molecules, for the QM and QM/MM simulation. Reference 16 reports an oxygen–oxygen rdf with a first peak at 2.8 Å. Its integration yields a value of 2.2 water molecules, fairly similar to our result. Notably, ref 18 obtains the rdf peaks at a slightly smaller distance (1.75 Å for hydrogen and 2.75 Å for oxygen), resulting in about one water molecule H bonded to formaldehyde; ref 17, instead, reports the peaks at 2.11 and 2.9 Å, respectively, again with one water molecule in the first solvation shell.

The specific influence of temperature effects on formaldehyde's structure and dipole is here investigated by comparing structural and electronic properties of **FA<sub>opt</sub>** with those of a CPMD simulation of formaldehyde in vacuo at 300 K (**FA<sub>CPMD</sub>**). The change in the CPMD-averaged C=O and C–H bond lengths with respect to those of **FA<sub>opt</sub>** is null or negligible. The average dipole moment is larger by about 24% (Table 1), showing a much smaller change than in **FA<sub>CPMD</sub><sup>aq</sup>** or **FA<sub>QMMM</sub><sup>aq</sup>**.

Temperature effects therefore do not cause a significant distortion to the structure of the molecule. The small number

of degrees of freedom of the system in **FA<sub>CPMD</sub>** does not allow for a proper dissipation of the thermal energy provided by the coupling to the thermostat. This provokes rather large fluctuations in the kinetic energy of formaldehyde (Figure S4 in the Supporting Information). As a consequence, the structure of the latter is particularly flexible.

We finally turn our attention to the vibrational spectrum. All vibrational frequencies, with the exception of the CH<sub>2</sub> rocking in **FA<sub>QMMM</sub><sup>aq</sup>**, are red shifted on going from **FA<sub>opt</sub>** to **FA<sub>CPMD</sub>**, **FA<sub>CPMD</sub><sup>aq</sup>**, and **FA<sub>QMMM</sub><sup>aq</sup>** (Table 2, Figure S3 in the Supporting Information). These comparisons should be taken with caution, since the vibrational frequencies for **FA<sub>opt</sub>** are calculated in a different way from those of **FA<sub>CPMD</sub><sup>aq</sup>** and **FA<sub>QMMM</sub><sup>aq</sup>** (see the Computational Methods section). In solution, the shift is more significant for the stretching modes (85–188 cm<sup>−1</sup>) than for the bending ones (14–98 cm<sup>−1</sup>). This contrasts with RIS-(CAS)SCF calculations,<sup>10</sup> which predict that the frequencies are shifted toward the blue, that is, the molecule becomes more rigid in the solvent. Early ab initio calculations of geometry-optimized complexes of H<sub>2</sub>CO...HO<sup>76</sup> suggest that solvation effects are qualitatively similar to our results, though the red shifts in this case are much smaller (within 40 cm<sup>−1</sup>). The effects of temperature can be clearly assessed also in the vibrational spectra: the shifts in **FA<sub>CPMD</sub>** are even larger than those of **FA<sub>CPMD</sub><sup>aq</sup>** and **FA<sub>QMMM</sub><sup>aq</sup>**. However, this might be due at least in part to scarce thermal energy dissipation.

In conclusion, the most important contribution of the solvent effects to structural, vibrational, and electronic properties is the polarization of the wave function, rather than the geometric distortion of formaldehyde. This is reflected by the remarkable change in the intensity of formaldehyde's dipole moment occurring between the gas phase and the solution case. As for temperature effects, these partially affect the vibrational spectrum of formaldehyde. The structure of the latter is more flexible than in the gas phase.

**First Electronic Excitation Energy.** TDDFT and CASPT2 approaches have been used to compute the electronic transition energy between the ground (S0) and the first excited state (S1). The latter is characterized by a single occupation of two orbitals. The *n* molecular orbital (HOMO) is localized on the oxygen and the π\* molecular orbital (LUMO) along the C=O double bond (Figure S1 in the Supporting Information).

The absorption energy values for the *n* → π\* transition (Δ*E*) of **FA<sub>opt</sub>**, calculated with TDDFT and CASPT2 methods, are similar (ranging from 3.82 to 3.85 eV). They do not depend on the functional used (BLYP or PBE). Thus, only BLYP calculations are reported here. The results are collected in Table 3, where we also report the values of the excitation energies obtained on the formaldehyde geometry optimized at the CASSCF level, showing a good agreement (within 0.04 eV) with the values obtained for **FA<sub>opt</sub>**. Our calculated values of Δ*E* at 0 K agree with other DFT,<sup>5,6</sup> coupled cluster,<sup>6</sup> CISD, and CASSCF<sup>13</sup> as well as with the experimental values of refs 21 and 22 (Table 3). The latter are measured from setups which keep formaldehyde at rather high temperatures (around 330 K). However, this is expected

**Table 5.** Literature Values of the Temperature- and Water-Induced Blue Shift of  $\Delta E$  (in eV)<sup>a</sup>

full QM approaches	QM/MM approaches	$\Delta E$
(IVC)-PCM//PCM opt PBE0(6-311++G(d,p))// TD-PBE0(6-311++G(d,p)) <sup>5</sup>		0.07–0.12
IEF-PCM//gpo CASSCF, MR-CI(6-31G**)// CASSCF, MR-CI(6-31G**) <sup>19</sup>	QM/MMpol//gpo AM1//CI <sup>4</sup>	0.14
FMO//FMO-HF(6-31G)//CIS(D)(6-31G*) <sup>16</sup>	RISM-SCF//gpo RHF(DZP)//CASSCF(DZP) <sup>9</sup>	0.15–0.2
	ASEP//gas phase exp//CASSCF(ANO) <sup>12</sup>	
	QM/classical//gpo MP2(ANO)// CASSI(ANO) <sup>17</sup>	
	ASEP//gpo MP2(cc-pvtz)//MRCI(cc-pvtz) <sup>18</sup>	
	effective potential//cluster opt HF(DZP)//MRD-CI(DZP) <sup>81</sup>	
	RISM-SCF//RISM-SCF opt CASSCF(DZP)// CASSCF(DZP) <sup>10</sup>	0.21–0.25
	QM/MM//gpo B3LYP(cc-pVTZ)// LR-CCSD(aug-cc-pVTZ) <sup>11</sup>	
QM//gpo MP2(aug-cc-pVDZ)//TDDFT(6-311++G(d,p)) <sup>7</sup>	ASEP//gpo RHF(6-31G+d)//CASPT2(6-311+G/G**) <sup>13</sup>	0.25–0.35
QM//INDO//CIS <sup>15</sup>	QM/MM//CCSD/MM(6-31++G), B3LYP/MM(6-31++G)// LR-CCSD(6-31++G), LR-B3LYP(6-31++G) <sup>6</sup>	
	QM/MM//gpo RHF(6-31G+d)//RHF(6-31G+d) <sup>8</sup>	
	QM/MM-pol-vib/CAV//gpo CCSD(TZ+2P)// CASSCF(cc-pVTZ) <sup>14</sup>	
dielectric continuum PBF//gas phase opt RHF(6-31G+d)// CIS(6-31G**) and dipolar coupling//gas phase opt RHF(6-31G+d)/CIS(6-31G**) <sup>20</sup>	QM/MM//gpo RHF(6-31G+d)//CIS(6-31G**) and dipolar coupling//gas phase opt RHF(6-31G+d)/CIS(6-31G**) <sup>20</sup>	0.43

<sup>a</sup> Details of the cited schemes used to incorporate the water environment in the calculations//theoretical methodologies and basis sets used for the calculation of solute geometries//and of the absorption energies. opt, geometry optimization of the system; gpo, gas-phase optimization: formaldehyde geometry was constrained to the gas-phase-optimized one.

not to have a significant effect on the absorption of formaldehyde in the UV range.

It was not possible to obtain the value of  $\Delta E$  for  $\mathbf{FA}_{\text{CPMD}}^{\text{aq}}$  with TDDFT, because of charge transfer between the solute and the solvent.<sup>77,78</sup> Indeed, all excitations we could compute with TDDFT on the  $\mathbf{FA}_{\text{CPMD}}^{\text{aq}}$  setup were localized on water molecules and not on formaldehyde.

The  $\Delta E$  values in solution as calculated with TDDFT, and, more, with CASPT2, are larger than those of  $\mathbf{FA}_{\text{opt}}$  (Table 4). The H-bond interactions between water and the solute oxygen in fact decrease the energy of the  $n$  state relative to  $\mathbf{FA}_{\text{opt}}$ , increasing  $\Delta E$ .<sup>79</sup> The predicted values are close to the experimental data<sup>23</sup> and a variety of calculations (Table 5). These are in the 3.5–5 eV range and predict a blue shift within 0.07–0.43 eV.

To disentangle temperature and wave function polarization contributions of the ground and excited state, we calculated  $n \rightarrow \pi^*$  excitation energies in vacuo also on the geometries of formaldehyde extracted from the MD simulation in water solution ( $\mathbf{FA}_{\text{CPMD}}^{\text{aq}}$  and  $\mathbf{FA}_{\text{QM/MM}}^{\text{aq}}$ ). Notably, the results are identical to those calculated from  $\mathbf{FA}_{\text{CPMD}}$  (compare the results reported in Tables 3 and 4). Hence, we attribute the whole blue shift to polarization of the wave functions of the two states.

An analogous consideration was raised in ref 80 for a similar molecule (acrolein) in water solution. However, in that case the distortion of geometry was nevertheless pointed out as a major factor of changes in the absorption spectra.

We do not find significant differences in the excitation energies obtained with CASPT2 over configurations obtained with full QM water and those from the mixed QM/MM

approach. This is justified by the small differences that we could detect in the structural features (geometry and dipole moment of formaldehyde, rdf of water around the carbonyl) of the systems described at the full QM and at the hybrid one.

Since geometry distortion plays no significant role in modifying the absorption energy of formaldehyde, the use of an explicit or implicit solvent model should bring the same result in terms of  $\Delta E$ . It is worth noticing that implicit solvent approaches, such as those of refs 5 and 19, predict rather small solvent blue shifts, with respect to those obtained from QM/MM techniques such as the LR-CCSD/MM of ref 11, the RISM-SCF approach of ref 10, and the CASPT2-ASEP of ref 13 as well as with respect to full QM calculations (the CIS of ref 15, and TDDFT calculations of ref 7). Adding polarizability to such schemes may result in enlarging the solvent shift values, as shown in ref 20. Nevertheless, molecular solvent schemes tend to produce higher shifts.<sup>20</sup>

In conclusion, we presented a Car–Parrinello QM and QM/MM MD study with excited-state calculations.

The geometry of formaldehyde, its normal modes, and its dipole moment in the gas phase agree with experiments<sup>70,71,75</sup> as well as with the past literature. The effects of solvent on these structural features, as known from previous calculations,<sup>10,14,18,68,69</sup> are also recovered with the simulations performed here.

The excitation energies calculated with both the TDDFT and the CASPT2 approaches are in good agreement with experimental and other theoretical results.<sup>9–13,17,18,81</sup> In particular, they predict a blue shift in the  $n \rightarrow \pi^*$  absorption energy that is here assigned to wave function polarization effects by the solvent.

**Supporting Information Available:** Brief summary of other studies about the absorption spectra of formaldehyde, along with further details about the analysis performed on the calculations presented in the main text of this article. This material is available free of charge via the Internet at <http://pubs.acs.org>.

## References

- (1) Guilbault, G. G. *Practical Fluorescence*, 2nd ed.; Marcel Dekker, Inc.: New York, 1990.
- (2) Öhrn, A.; Karlström, G. *J. Phys. Chem. A* **2006**, *110*, 1934–1942.
- (3) Improta, R.; Scalmani, G.; Frisch, M. J.; Barone, V. *J. Chem. Phys.* **2007**, *127*, 074504–074513.
- (4) Thompson, M. A. *J. Phys. Chem.* **1996**, *100*, 14492–14507.
- (5) Cossi, M.; Barone, V. *J. Chem. Phys.* **2001**, *115*, 4708–4718.
- (6) Nielsen, C. B.; Christiansen, O.; Mikkelsen, K. V.; Kongsted, J. *J. Chem. Phys.* **2007**, *126*, 154112–154130.
- (7) Malaspina, T.; Coutinho, K.; Canuto, S. *J. Braz. Chem. Soc.* **2008**, *19*, 305–311.
- (8) Blair, J. T.; Krogh-Jespersen, K.; Levy, R. M. *J. Am. Chem. Soc.* **1989**, *111*, 6948–6956.
- (9) Ten-no, S.; Hirata, F.; Kato, S. *J. Chem. Phys.* **1994**, *100*, 7443–7454.
- (10) Naka, K.; Morita, A.; Kato, S. *J. Chem. Phys.* **1999**, *110*, 3484–3493.
- (11) Kongsted, J.; Osted, A.; Mikkelsen, K. V.; Astrand, P.-O.; Christiansen, O. *J. Chem. Phys.* **2004**, *121*, 8435–8446.
- (12) Martín, M. E.; Sánchez, M. L.; del Valle, F. J. O.; Aguilar, M. A. *J. Chem. Phys.* **2000**, *113*, 6308–6315.
- (13) Sánchez, M. L.; Martín, M. E.; Aguilar, M. A.; Olivares del Valle, F. J. *Chem. Phys. Lett.* **1999**, *310*, 195–200.
- (14) Kawashima, Y.; Dupuis, M.; Hirao, K. *J. Chem. Phys.* **2002**, *117*, 248–258.
- (15) Coutinho, K.; Saavedra, N.; Serrano, A.; Canuto, S. *J. Mol. Struct.: THEOCHEM* **2001**, *539*, 171–179.
- (16) Mochizuki, Y.; Komeiji, Y.; Ishikawa, T.; Nakano, T.; Yamataka, H. *Chem. Phys. Lett.* **2007**, *437*, 66–72.
- (17) Öhrn, A.; Karlström, G. *Mol. Phys.* **2006**, *104*, 3087–3099.
- (18) Xu, Z.; Matsika, S. *J. Phys. Chem. A* **2006**, *110*, 12035–12043.
- (19) Mennucci, B.; Cammi, R.; Tomasi, J. *J. Chem. Phys.* **1998**, *109*, 2798–2808.
- (20) Bader, J. S.; Cortis, C. M.; Berne, B. J. *J. Chem. Phys.* **1997**, *106*, 2372–2388.
- (21) Walzl, K. N.; Koerting, C. F.; Kuppermann, A. *J. Chem. Phys.* **1987**, *87*, 3796–3803.
- (22) Taylor, S.; Wilden, D. G.; Comer, J. *J. Chem. Phys.* **1982**, *70*, 291–298.
- (23) Bercovici, T.; King, J.; Becker, R. *J. Chem. Phys.* **1972**, *56*, 3956–3963.
- (24) Röhrig, U. F.; Frank, I.; Hutter, J.; Laio, A.; VandeVondele, J.; Röthlisberger, U. *ChemPhysChem* **2003**, *4*, 1177–1182.
- (25) Conte, A. M.; Ippoliti, E.; Del Sole, R.; Carloni, P.; Pulci, O. *J. Chem. Theory Comput.* **2009**, *5*, 1822–1828.
- (26) Sulpizi, M.; Carloni, P.; Hutter, J.; Röthlisberger, U. *Phys. Chem. Chem. Phys.* **2003**, *5*, 4798–4805.
- (27) Murugan, N. A.; Rinkevicius, Z.; Ågren, H. *J. Phys. Chem. A* **2009**, *113*, 4833–4839.
- (28) Spezia, R.; Duvail, M.; Vitorge, P.; Cartailier, T.; Tortajada, J.; Chillemi, G.; D'Angelo, P.; Gaigeot, M. P. *J. Phys. Chem. A* **2006**, *110*, 13081–13088.
- (29) Tilocca, A.; Fois, E. *J. Phys. Chem. C* **2009**, *113*, 8683–8687.
- (30) Hutter, J. *J. Chem. Phys.* **2003**, *118*, 3928–3935.
- (31) Andersson, K.; Malmqvist, P. Å.; Roos, B. O. *J. Chem. Phys.* **1992**, *96*, 1218–1226.
- (32) Liao, D.-W.; Mebel, A. M.; Chen, Y.-T.; Lin, S.-H. *J. Phys. Chem. A* **1997**, *101*, 9925–9934.
- (33) Muñoz Losa, A.; Fdez.-Galván, I.; Aguilar, M. A.; Martín, M. E. *J. Phys. Chem. B* **2007**, *111*, 9864–9870.
- (34) Serrano-Andrés, L.; Fülcher, M. P.; Karlström, G. *Int. J. Quantum Chem.* **1997**, *65*, 167–181.
- (35) Hohenberg, P.; Kohn, W. *Phys. Rev.* **1964**, *136*, B864–B871.
- (36) Kohn, W.; Sham, L. J. *Phys. Rev.* **1965**, *140*, A1133–A1138.
- (37) Becke, A. *Phys. Rev. A* **1988**, *38*, 3098–3100.
- (38) Lee, C.; Yang, W.; Parr, R. *Phys. Rev. B* **1988**, *37*, 785–789.
- (39) Piana, S.; Carloni, P. *Proteins* **2000**, *39*, 26–36.
- (40) Bucher, D.; Guidoni, L.; Carloni, P.; Röthlisberger, U. *Biophys. J.* **2010**, *98*, L47–L49.
- (41) Alves, C. N.; Martí, S.; Castillo, R.; Andrés, J.; Moliner, V.; Tuóú, I.; Silla, E. *Bioorg. Med. Chem.* **2007**, *15*, 3818–3824.
- (42) Bucher, D.; Raugei, S.; Guidoni, L.; Dal Peraro, M.; Röthlisberger, U.; Carloni, P.; Klein, M. L. *Biophys. Chem.* **2006**, *124*, 292–301.
- (43) Perdew, J. P.; Burke, K.; Ernzerhof, M. *Phys. Rev. Lett.* **1996**, *77*, 3865–3868.
- (44) Ernzerhof, M.; Scuseria, G. E. *J. Chem. Phys.* **1999**, *110*, 5029–5037.
- (45) Troullier, N.; Martins, J. L. *Phys. Rev. B* **1991**, *43*, 1993–2006.
- (46) Kleinman, L.; Bylander, D. M. *Phys. Rev. Lett.* **1982**, *48*, 1425–1428.
- (47) von Lilienfeld, O.; Tavernelli, I.; Röthlisberger, U.; Sebastiani, D. *Phys. Rev. Lett.* **2004**, *93*, 153004–153008.
- (48) Császár, P.; Pulay, P. *J. Mol. Struct.* **1984**, *114*, 31–34.
- (49) Jorgensen, W.; Chandrasekhar, J.; Madura, J.; Impey, R.; Klein, M. *J. Chem. Phys.* **1983**, *79*, 926–936.
- (50) Quigley, D.; Probert, M. *J. Chem. Phys.* **2004**, *120*, 11432–11442.
- (51) Wang, J.; Cieplak, P.; Kollman, P. A. *J. Comput. Chem.* **2000**, *21*, 1049–1074.
- (52) Ryckaert, J.; Ciccotti, G.; Berendsen, H. *J. Comput. Phys.* **1977**, *23*, 327–341.
- (53) Essmann, U.; Perera, L.; Berkowitz, M.; Darden, T.; Lee, H.; Pedersen, L. *J. Chem. Phys.* **1995**, *103*, 8577–8594.
- (54) Phillips, J.; Braun, R.; Wang, W.; Gumbart, J.; Tajkhorshid, E.; Villa, E.; Chipot, C.; Skeel, R.; Kalé, L.; Schulten, K. *J. Comput. Chem.* **2005**, *26*, 1781–1802.

- (55) Martyna, G.; Tuckerman, M. *J. Chem. Phys.* **1999**, *110*, 2810–2922.
- (56) Hoover, W. *Phys. Rev. A* **1985**, *31*, 1695–1697.
- (57) CPMD, version 3.13.2; IBM Corp. 1990–2008, MPI für Festkörperforschung Stuttgart 1997–2001, 2009; <http://www.cpmc.org/>.
- (58) Silvestrelli, P. L.; Marzari, N.; Vanderbilt, D.; Parrinello, M. *Solid State Commun.* **1998**, *107*, 7–11.
- (59) Marzari, N.; Vanderbilt, D. *Phys. Rev. B* **1997**, *56*, 12847–12865.
- (60) Wilson, E.; Decius, J.; Cross, P. C. *Molecular Vibrations: The Theory of Infrared and Raman Vibrational Spectra*; Dover Publications Inc.: Mineola, NY, 1980.
- (61) Carloni, P.; Sprik, M.; Andreoni, W. *J. Phys. Chem. B* **2000**, *104*, 823–835.
- (62) Runge, E.; Gross, E. *Phys. Rev. Lett.* **1984**, *52*, 997–1000.
- (63) Casida, M. E. Time-Dependent Density Functional Response Theory for Molecules. In *Recent Advances in Density Functional Methods*; Chong, D. P., Ed.; World Scientific: Singapore, 1995; Vol. 1, Chapter 5, pp 155–192.
- (64) Widmark, P.-O.; Malmqvist, P.-Å.; Roos, B. O. *Theor. Chim. Acta* **1990**, *77*, 291–306.
- (65) Altoé, P.; Stenta, M.; Bottoni, A.; Garavelli, M. *Theor. Chim. Acta* **2007**, *118*, 219–240.
- (66) van Gunsteren, W. F.; Billeter, S. R.; Eising, A. A.; Hunenberger, P. H.; Kroger, P.; Mark, A. E.; Scott, W. R. P.; Tironi, I. G. *Biomolecular Simulation: The GROMOS96 Manual and User Guide*; Vdf Hochschulverlag AG an der ETH Zurich: Zurich, 1996.
- (67) Karlstrom, G.; Lindh, R.; Malmqvist, P.; Roos, B.; Ryde, U.; Veryazov, V.; Widmark, P.; Cossi, M.; Schimmelpfennig, B.; Neogrady, P.; Seijo, L. *Comput. Mater. Sci.* **2003**, *28*, 222–239.
- (68) Jalbouda, A. F.; El-Nahas, A. M. *J. Mol. Struct.: THEOCHEM* **2004**, *671*, 125–132.
- (69) George, W.; Jones, B.; Lewisa, R.; Pricea, J. *J. Mol. Struct.* **2000**, *550–551*, 281–296.
- (70) Takagi, K.; Oka, T. *J. Phys. Soc. Jpn.* **1963**, *18*, 1174–1180.
- (71) Moule, D. C.; Walsh, A. D. *Chem. Rev.* **1975**, *75*, 67–84.
- (72) Schoolery, J. N.; Sharbaugh, A. H. *Phys. Rev.* **1951**, *82*, 95–95.
- (73) Garavelli, M.; Negri, F.; Olivucci, M. *J. Am. Chem. Soc.* **1999**, *121*, 1023–1029.
- (74) Bernal, R.; Lemus, R. *J. Mol. Spectrosc.* **2006**, *235*, 218–234.
- (75) Job, V. A.; Sethuraman, V.; Innes, K. K. *J. Mol. Spectrosc.* **1969**, *30*, 365–426.
- (76) Dimitrova, Y. *J. Mol. Struct.: THEOCHEM* **1997**, *391*, 251–257.
- (77) Röthlisberger, U.; Carloni, P. Drug-Target Binding Investigated by Quantum Mechanical/Molecular Mechanical (QM/MM) Methods. In *Computer Simulations in Condensed Matter Systems: From Materials to Chemical Biology*; Ferrario, M., Ciccotti, G., Binder, K., Eds.; Springer Berlin/Heidelberg: Berlin, Heidelberg, 2006; Vols. 2 and 704, Chapter 17, pp 449–479.
- (78) Dal Peraro, M.; Raugei, S.; Carloni, P.; Klein, M. L. *ChemPhysChem* **2005**, *6*, 1715–1718.
- (79) Bayliss, N. S.; McRae, E. G. *J. Phys. Chem.* **1954**, *58*, 1002–1006.
- (80) Martín, M. E.; Losa, A. M.; Fdez.-Galván, I.; Aguilar, M. A. *J. Chem. Phys.* **2004**, *121*, 3710–3717.
- (81) Frank, I.; Grimme, S.; von Arnim, M.; Peyerimhoff, S. D. *Chem. Phys.* **1995**, *199*, 145–153.

CT100384F